

Green Chemistry

Accepted Manuscript



This is an *Accepted Manuscript*, which has been through the Royal Society of Chemistry peer review process and has been accepted for publication.

Accepted Manuscripts are published online shortly after acceptance, before technical editing, formatting and proof reading. Using this free service, authors can make their results available to the community, in citable form, before we publish the edited article. We will replace this *Accepted Manuscript* with the edited and formatted *Advance Article* as soon as it is available.

You can find more information about *Accepted Manuscripts* in the [Information for Authors](#).

Please note that technical editing may introduce minor changes to the text and/or graphics, which may alter content. The journal's standard [Terms & Conditions](#) and the [Ethical guidelines](#) still apply. In no event shall the Royal Society of Chemistry be held responsible for any errors or omissions in this *Accepted Manuscript* or any consequences arising from the use of any information it contains.

An environmentally benign, mild, and catalyst-free reaction of quinones with heterocyclic ketene aminals in ethanol: site-selective synthesis of rarely fused [1,2-*a*]indolone derivatives *via* an unexpected anti-Nenitzescu strategy†

Cite this: DOI: 10.1039/c4gc00000x

Bei Zhou,^{†a} Zhi-Cheng Liu,^{†a,b} Wen-Wen Qu,^b Rui Yang,^b Xin-Rong Lin,^a Sheng-Jiao Yan,^{*a} and Jun Lin^{*a}

As a classical and well-established named reaction, the Nenitzescu reaction is of special value for the construction of biologically meaningful 5-hydroxyindole derivatives. However, to date, its sister, the anti-Nenitzescu reaction and corresponding synthetic methodology for 3a-hydroxy-indol-6-one derivatives, remains an uncultivated land. We discovered herein an environmentally benign, mild, and catalyst-free reaction in ethanol for the site-selective construction of rarely fused [1,2-*a*]indolone derivatives (**3**) from quinones (**1**) and heterocyclic ketene aminals (HKAs) (**2**) *via* an unexpected anti-Nenitzescu strategy. This unconventional methodology suggests that it will be suitable for the site-selective synthesis of 3a-hydroxy-indol-6-one derivatives from a green perspective. On the other hand, the developed target compounds **3** have a promising future for the further synthesis of aromatic 6-hydroxyindoles or dehydroxylated indol-6-ones *in situ*. In order to systematically elucidate the mechanistic details and controlling factors of the two Nenitzescu reactions, density functional theory (DFT) calculations were also performed. According to the computational results, the origin of site-selectivity can be explained by following reasons: all energy barriers for the anti-Nenitzescu reaction can be overcome at room temperature, yet the extremely high energy barrier of imine-enamine tautomerization for the Nenitzescu reaction indicates its failure under the same conditions. The reduced density gradient (RDG) analysis hinted that the greater thermodynamic stability of the Nenitzescu product **3h'** mainly depends on the release of the strong steric effect.

Received 14th April 2014,
Accepted XXth July 2014

DOI: 10.1039/c4gc00000x

www.rsc.org/greenchem

Introduction

In organic chemistry, the ideal synthesis¹ should be a combination of a number of environmental, health, safety, and economic targets, which obviously requires a rational design of the complex and functionalized targets based on fundamental

^a Key Laboratory of Medicinal Chemistry for Natural Resource (Yunnan University), Ministry of Education, School of Chemical Science and Technology, Yunnan University, Kunming, 650091, P. R. China. Fax: +86 871 65033215; Tel: +86 871 65033215; E-mail: yansj@ynu.edu.cn; linjun@ynu.edu.cn

^b Department of Applied Chemistry, Faculty of Science, Kunming University of Science and Technology, Kunming, 650500, P. R. China.

†Electronic Supplementary Information (ESI) available: ¹H and ¹³C spectra of all new compounds. 2D NMR spectra of compound **3o**. HPLC profile. Computational data for geometries and energies of all optimized structures. For ESI or other electronic format see DOI: 10.1039/c4gc00000x

‡These authors contributed equally to this paper.

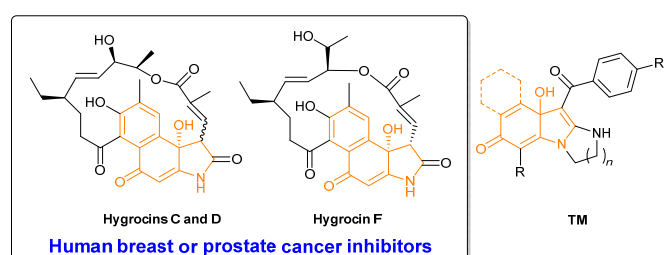


Fig. 1 Naturally occurring compounds with 3a-hydroxy-indol-6-one nucleus.

understanding to address several green chemistry principles in a comprehensive manner.² In fact, selective and efficient construction of C–C and C–N bonds is of significant interest to organic synthesis because nitrogen-containing products find a plethora of applications in the chemistry of medicinal and natural

products as well as life science.³ As a class of important and well-known heterocyclic scaffolds, indoles are embedded in many biological systems and present extremely intriguing applications in medicine, agriculture, materials and chemical industry.⁴ Nonetheless, an uncommon indole nucleus, 3a-hydroxy-indol-6-one has very rarely been investigated regarding its discovery and synthesis. Currently, to the best of our knowledge, no information is available for the synthesis of 3a-hydroxy-indol-6-one derivatives, and only one example is known for the separation of cytotoxic ansamycins from *Streptomyces* sp. LZ35 by Lu *et al* (Fig. 1).⁵ This finding offers straightforward evidence for the existence of the 3a-hydroxy-indol-6-one nucleus in nature. Accordingly, this perspective defines the aim of our study, *i.e.* to synthesize derivatives which contain a 3a-hydroxy-indol-6-one nucleus from a green vision.

In the past few decades, stereoselective and regioselective synthesis focusing on heterocycles that are frequently found in natural products, pharmaceuticals, and dyes has played a significant role in many chemical branches, leading to the rapid development of widely used synthons, *i.e.*, heterocyclic ketene animals (HKAs), for concise and efficient access to highly functionalized target materials. As interest in HKA-related transformations is steadily growing, several attractive HKA-based heterocyclic skeletons and fused heterocycles, including indoles,⁶ quinolines,⁷ naphthyridines,⁸ 1,2,3-triazoles,⁹ coumarins,¹⁰ as well as pyridines,¹¹ pyrimidines,¹² and perimidines¹³ have been constructed (Fig. 2). Although HKAs can serve as polyfunctional synthons,¹⁴ their application in the green synthesis of structurally and biologically meaningful heterocycles is still in the burgeoning phase.

The Nenitzescu reaction is a classical named reaction,¹⁵ which affords 5-hydroxyindole derivatives by the condensation of 1,4-benzoquinones with enamines.¹⁶ Although the starting

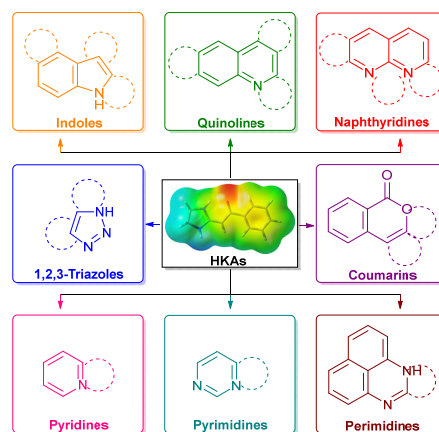
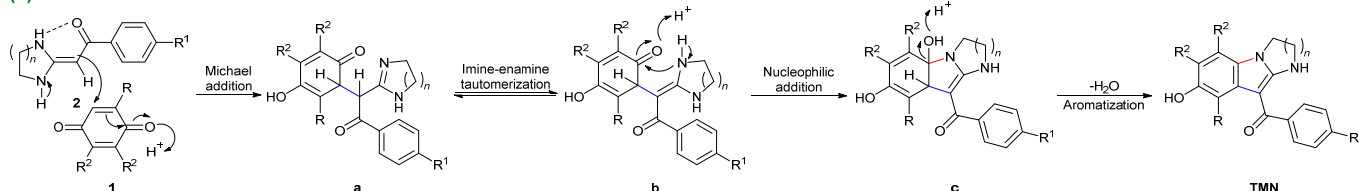


Fig. 2 Molecular diversity of HKAs based heterocyclic skeletons and fused heterocycles.

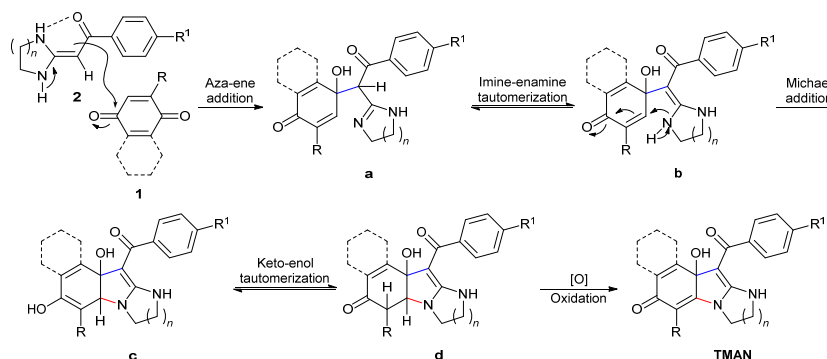
materials for the reaction are simple and readily accessible, the isolated yields are quite low due to side reactions. Therefore, to overcome this limitation,¹⁷ in our prior study,^{6c} we maximally improved the yields (up to 93%) of the classical reaction by employing HKAs as enamines in boiling 1,4-dioxane. Nevertheless, the shortcomings of the reaction in terms of green aspects were toxic solvents, prolonged reflux, and the requirement for purification by column chromatography.

Hence, to develop a greener synthetic methodology with benign conditions, less time, straightforward post-treatments, and high yields, we designed herein a catalyst-free reaction of quinones (**1**) with HKAs (**2**) in ethanol at room temperature. Surprisingly, the nucleus of the target material (**3**) was an unexpected 3a-hydroxyindol-6-one, and the outcome can be considered as a highly site-selective anti-Nenitzescu strategy. Actually, the mechanism of the transformation disobeys the widely recognized convention. Instead, the sequence is: (i) aza-

(a) Nenitzescu Process



(b) Anti-Nenitzescu Process



Scheme 1 Proposed mechanism for the sister Nenitzescu reactions which derived from quinones **1** with HKAs **2**.

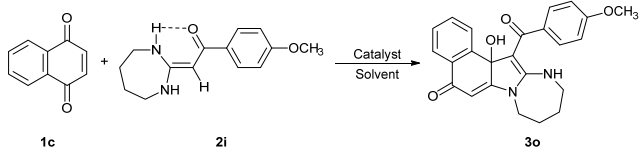
ene addition → (ii) imine-enamine tautomerization → (iii) Michael addition → (iv) keto-enol tautomerization → (v) oxidation (Scheme 1).

Moreover, considering the excellent site-selectivity and unconventional mechanism, it is imperative to develop a mechanistic understanding of the two reactions. Thus, we also carried out here a joint computational study to shed light on the location of possible stationary structures along with their reaction pathways, energy profiles, and solvent effects based on density functional theory (DFT).¹⁸ It is our belief that the expanded theoretical investigation will yield valuable clues and determine how this exception occurs. This will avoid a futile waste of time and resources by taking the experiment into cyberspace and furthermore greatly advance green chemistry.

Results and discussion

Initially, the reaction between an equimolar ratio of naphthalene-1,4-dione (**1c**) and HKA (**2i**) was chosen as a model reaction for the optimization of reaction conditions. By performing the reaction in the presence of equivalent acidic or basic catalyst and an aprotic solvent (1,4-Dioxane) at room temperature for 10 minutes (Table 1, entries 1–5), the weak organic base Et₃N was found to be a promising catalyst for the synthesis of indolone **3o**. Subsequently, we screened several aprotic or protonic solvents with variable polarity (Table 1, entries 6–12). The results revealed that the most suitable solvent for this transformation was anhydrous ethanol. Obviously, the polarity of the solvents had a certain influence on the yield of **3o**. Next, to search for greener conditions, we tested the reaction under catalyst-free condition (Table 1, entries 13–16). Unexpectedly, the prospective product **3o** could

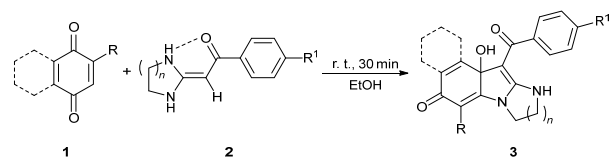
Table 1 Optimization of the reaction conditions for the model reaction^a



Entry	Catalyst	Solvent	Time (min)	Yield ^b (%)
1	HOAc	1,4-Dioxane	10	N. R.
2	Et ₃ N	1,4-Dioxane	10	30
3	K ₂ CO ₃	1,4-Dioxane	10	N. R.
4	DBU	1,4-Dioxane	10	26
5	EtONa	1,4-Dioxane	10	trace
6	Et ₃ N	CH ₂ Cl ₂	10	36
7	Et ₃ N	THF	10	48
8	Et ₃ N	CH ₃ CN	10	50
9	Et ₃ N	Toluene	10	trace
10	Et ₃ N	EtOH	10	55
11	Et ₃ N	H ₂ O	10	24
12	Et ₃ N	H ₂ O/EtOH (1:1, v:v)	10	26
13	–	H ₂ O	10	20
14	–	H ₂ O/EtOH (1:1, v:v)	10	38
15	–	EtOH	10	61
16	–	EtOH	30	95

^a Reaction conditions: **1c** (1.1 mmol) was dissolved in the solvent (10 mL) and added dropwise to the mixture of **2i** (1.0 mmol), catalyst (1.0 mmol), and solvent (15 mL). ^b Isolated yield based on HKA **2i**. N. R. = no reaction.

Table 2 Substrate scope of the quinones **1** and HKAs **2**^a



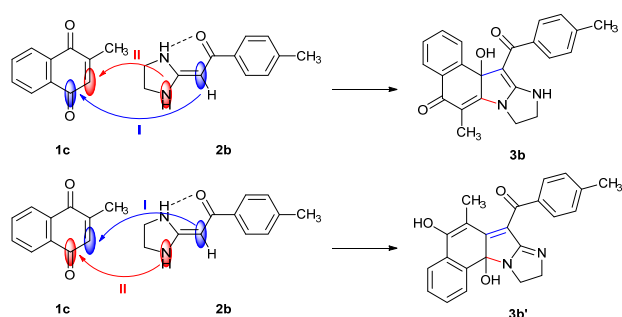
Entry	1 (R/Ring)	2 (n/R ¹)	3	Yield ^b (%)
1	1c (CH ₃ /Ph)	2a (1/OCH ₃)	3a	78
2	1c (CH ₃ /Ph)	2b (1/CH ₃)	3b	80
3	1c (CH ₃ /Ph)	2d (1/Cl)	3c	79
4	1d (H/Naph)	2b (1/CH ₃)	3d	90
5	1d (H/Naph)	2c (1/H)	3e	85
6	1d (H/Naph)	2d (1/Cl)	3f	92
7	1a (H/–)	2f (2/CH ₃)	3g	96
8	1a (H/–)	2g (2/H)	3h	98
9	1b (H/Ph)	2e (2/OCH ₃)	3i	93
10	1b (H/Ph)	2f (2/CH ₃)	3j	90
11	1b (H/Ph)	2g (2/H)	3k	92
12	1b (H/Ph)	2h (2/Cl)	3l	94
13	1c (CH ₃ /Ph)	2g (2/H)	3m	78
14	1d (H/Naph)	2f (2/CH ₃)	3n	92
15	1b (H/Ph)	2i (3/OCH ₃)	3o	98
16	1b (H/Ph)	2j (3/CH ₃)	3p	96
17	1b (H/Ph)	2k (3/H)	3q	95
18	1b (H/Ph)	2l (3/Cl)	3r	95
19	1d (H/Naph)	2j (3/CH ₃)	3s	96
20	1d (H/Naph)	2k (3/H)	3t	93
21	1d (H/Naph)	2l (3/Cl)	3u	95

^a Synthesis of target compounds **3**: **1** (1.1 mmol) dissolved in ethanol (10 mL) and added dropwise to the ethanolic solution (15 mL) of **2** (1.0 mmol); the mixture was stirred at room temperature for 30 minutes. ^b Isolated yield based on HKAs **2**.

be obtained with 95% yield when the time of the reaction was prolonged to 30 minutes. Therefore, it could be concluded that the optimum conditions for the synthesis of **3o** were anhydrous ethanol as the solvent with no catalyst at room temperature for 30 minutes (Table 1, entry 16).

Once the optimized conditions had been developed, we examined the substrate scope of the anti-Nenitzescu reaction (Table 2). The formulated system was tolerant to rings and functional groups (R) in quinones **1**. For the quinone ring, with an increase in the size, *viz.*, benzoquinone → naphthoquinone → anthraquinone, the yields of **3** decreased in turn (*e.g.* Table 2, entries 8, 11, and 14). This observation hinted that the rigidity of **1** determines the intensity of ring strain between the quinone motif and the diazaheterocycle.

In addition, when a methyl was introduced to the α -position of **1**, the yields of **3** decreased (*e.g.* Table 2, entries 11 and 18). In order to investigate the main reason for this, the resulting crude products¹⁹ of representative substrates **1c** and **2b** were subjected to separation by preparative high pressure liquid chromatography (HPLC) on a reverse-phase C18 column (CH₃CN, 0–100%) to yield two fractions (Fig. S49, ESI†). Fraction A (**3b**, peak area: 56%) was characterized as an anti-Nenitzescu result and fraction B (**3b'**, peak area: 23%) was a Nenitzescu product (Scheme 2). This finding served as direct

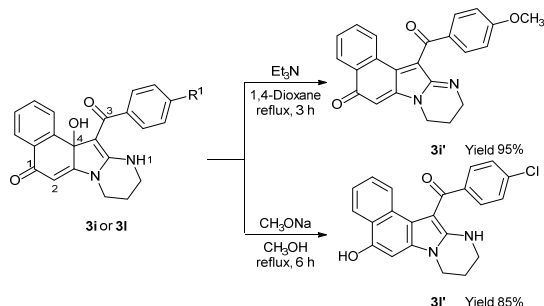


Scheme 2 Competition between the unconventional and classical Nenitzescu reaction in one-pot.

evidence that explained the decrease in the yield of **3b**, *i.e.*, it was primarily caused by the production of by-product **3b'**. Of course, from another point of view, it was shown that competition between the two types of the reaction, namely, classical Nenitzescu and anti-Nenitzescu, always occurred with the generation of asymmetry and a corresponding change in the electron density of the quinone ring.

Subsequently, we examined the compatibility of HKAs **2**. It was observed that the substituent group (R^1) on the aryl ring of **2** had an uncertain influence on the yields of **3**. However, the size of the diazaheterocycle of **2** showed that the seven-membered ring provided the highest yields, then the six-membered, and then the five-membered ring (*e.g.* Table 2, entries 4, 14, and 19). In this way, the general principle of fused ring strains between the indolone motif and the diazaheterocycle could be logically deduced as the following sequence: diazepino[1,2-*a*]indolone < pyrimido[1,2-*a*]indolone < imidazo[1,2-*a*]indolone.

Since the conventional Nenitzescu by-product **3b'** was successfully separated in a one-pot reaction, we suspected that the non-aromatic indolone could transform into an aromatic 6-hydroxyindole by elimination of the hydroxyl group. To actualize the proposed idea, product **3i** was refluxed with a strong organic base (CH_3ONa) in a protic solvent (methanol) for 6 hours. To our delight, the transformation of compound **3i** to **3i'** was successful and the yield of the target material **3i'** was 85% (Scheme 3). Contrasting the ^{13}C NMR spectra of compounds **3i** and **3i'** revealed that, once the transformation occurred, (i) for **3i**, signals for one of the two carbonyl groups (C1, δ : 182.4 ppm) and the non-aromatic methyne group (C2, δ :



Scheme 3 Two examples for the transformation of compounds **3i** and **3i'**.

106.3 ppm) disappeared; (ii) for **3i'**, the signal for the other carbonyl group (C3, δ : 187.2 ppm) remained in the same place and the newly generated aromatic methyne group (C2, δ : 101.8 ppm) was better shielded, hence the resonance signal was in a higher field; (iii) the elimination of the hydroxyl group caused a low-field shift in the quaternary carbon (C4, δ : 88.6 \rightarrow 135.7 ppm). It is clear that this synthetic strategy offers an alternative example to constructing 6-hydroxyindole architectures from a unique starting point.

Having completed the synthesis of compound **3i'**, we turned our attention to investigating another formal transformation for preparing the other target material (**3i'**), with excellent solubility in water, ethanol, *etc.* The combination of the base and the solvent, *i.e.*, Et_3N and 1,4-dioxane, was selected for the transformative synthesis of **3i'** from **3i** because Et_3N affords weak intensity and 1,4-dioxane provides an aprotic environment. In principle, the base ensured that deprotonation and elimination occurred; at the same time, the aprotic solvent blocked the protonation of the 6-carbonyl group as well. Consequently, the other direction for highly efficient elimination of the hydroxyl group was established and the yield of the target material **3i'** was up to 95% (Scheme 3). Similarly, after comparing the NMR spectra of compounds **3i** and **3i'**, the main alternation in the characteristic peaks was the low-field shift of the quaternary carbon (C4, δ : 88.5 \rightarrow 149.9 ppm) and the disappearance of the signal for NH (H1, δ : 9.61 ppm). Overall, this example is interesting because of its concise synthesis, intrinsic selectivity, and excellent bioavailability.

It is also worth noting that the procedure for the purification of all target products **3** only required recrystallization rather than column chromatography. This easy post-treatment protocol makes this methodology facile, practical, and rapid to execute.

All compounds were unambiguously characterized by IR, ^1H NMR, ^{13}C NMR, and HRMS spectroscopy. Full assignment of the ^1H and ^{13}C NMR chemical shifts and structural elucidation of compound **3o** were ascertained by evaluating the gHSQC, gCOSY, gNOESY, and gHMBC spectra. As an example, in the HMBC spectrum (Fig. 3), the carbonyl carbons (C1 and C2) showed strong $^3J_{\text{C-H}}$ -correlations to the protons H1, H1', and H2; the quaternary carbon C3 displayed $^3J_{\text{C-H}}$ -correlations to the protons H3 and H4; the aromatic carbons (C4 and C5) exhibited strong $^3J_{\text{C-H}}$ -correlations as well as $^2J_{\text{C-H}}$ -correlations to the protons H5, H5', H1, and H1'; the quaternary carbon C6 correlated with the protons H2, H7, and H8; additionally, the quaternary carbon C7 correlated with the protons H7, H9, and

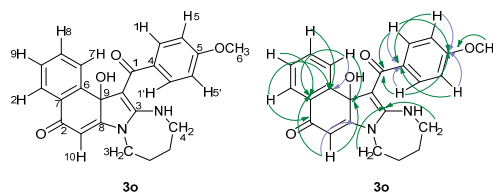


Fig. 3 Important HMBC correlations of compound **3o** (green arrows, $^3J_{\text{C-H}}$; light blue arrows, $^2J_{\text{C-H}}$).

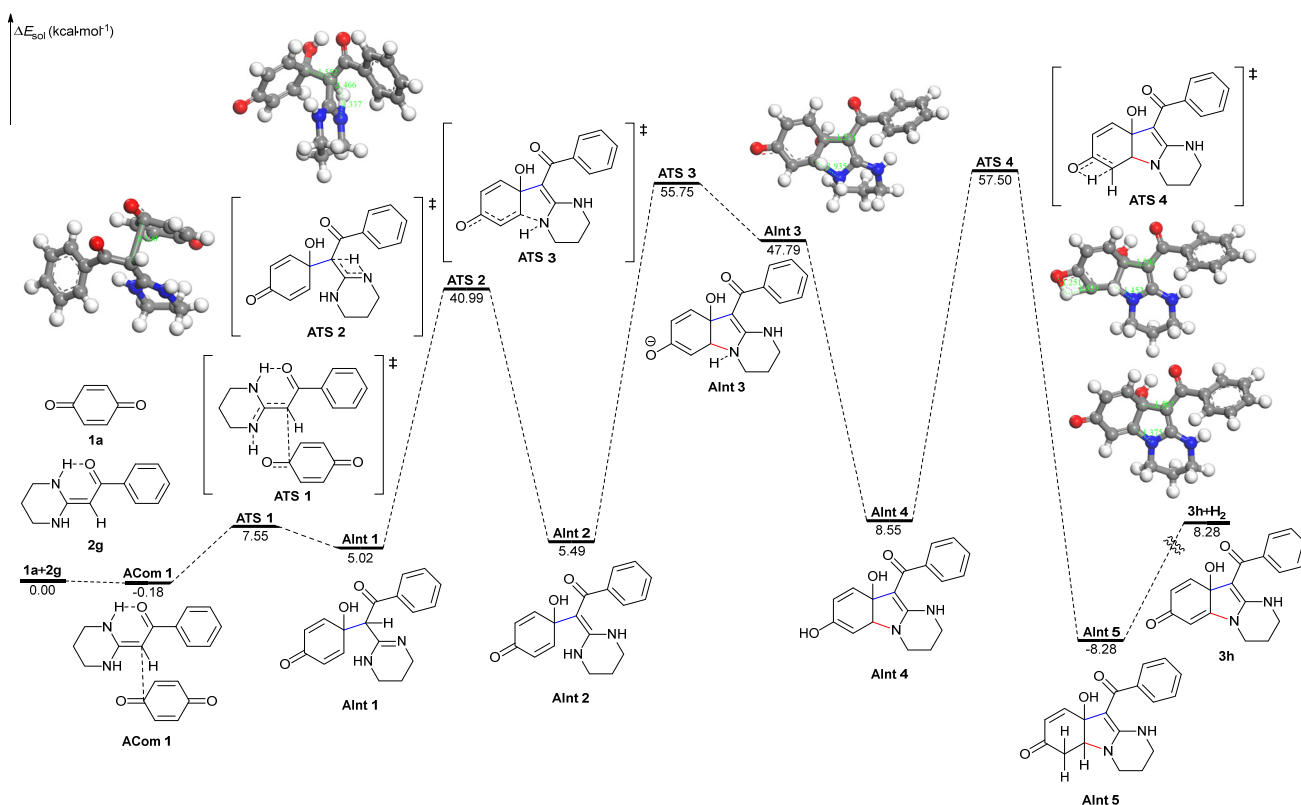


Fig. 4 Computed potential energy surface of the anti-Nenitzescu reaction between **1a** and **2g** at the m06/6-311+G(2d,2p)+ZPE[m06/6-31+G(d)] level. Relative energies (ΔE_{sol}), are with respect to **1a+2g** and are given in kcal·mol⁻¹.

H10; furthermore, the quaternary carbon C8, which was connected to the diazaheterocycle, presented strong ${}^2J_{\text{C-H}}$ -correlations to the proton H10; most importantly, the quaternary carbon C9 afforded strong ${}^3J_{\text{C-H}}$ -correlations to the protons H7 and H10.

DFT computations were conducted which shed light on the mechanism and site-selectivity of the two Nenitzescu reactions. At first, we focused on the model anti-Nenitzescu reaction of **1a** with **2g** in ethanol (Fig. 4). From the substrate coordinated complex **ACom 1**, the formation of a C–C bond *via* **ATS 1** required a relatively low energy barrier of 7.73 kcal·mol⁻¹ to generate the imine intermediate **AInt 1**. Afterward, intermediate **AInt 1** underwent imine-enamine tautomerization of 35.97 kcal·mol⁻¹ to form an enamine intermediate **AInt 2**. Then, the C–N bond formation step required an energy barrier of 50.26 kcal·mol⁻¹ (**AInt 2** → **ATS 3**); this was the rate-determining step. The transition state **ATS 3** demanded a 42.53 kcal·mol⁻¹ higher energy barrier than **ATS 1**, indicating that Michael addition is more difficult than the formation of a C–C bond. The further keto-enol tautomerization of enolic intermediate **AInt 4** needed an energy barrier of 48.95 kcal·mol⁻¹, leading to the corresponding keto form intermediate **AInt 5**. Finally, through a complex oxidation process, the anti-Nenitzescu target material **3h** was produced.

We also considered the model Nenitzescu reaction of **1a'** with **2g** in 1,4-dioxane which involved the opposite sequence of

attack (Fig. 5). The initial C–C bond formation pathway (**BCom 1** → **BTS 1**) required a very small energy barrier of 1.34 kcal·mol⁻¹, 6.39 kcal·mol⁻¹ lower than the addition of **2g** to **1a**. The energy barrier of the following imine-enamine tautomerization for path B (309.86 kcal·mol⁻¹) was 8.6 times higher than the corresponding step of path A. At the same time, in path B, the generation of enamine intermediate **BInt 3** was shown to be the most crucial, and therefore, it could also be recognized as the rate-determining step. Because of the extremely high energy barrier, the reaction could not proceed in an acidic environment at room temperature. Once the energy barrier of **BTS 2** was surmounted, the formation of the C–N bond required a relatively low energy barrier of 13.79 kcal·mol⁻¹ (**BInt 4** → **BTS 3**). In order to complete the aromatization, intermediate **BInt 6** was first dehydroxylated to form the active carbocation intermediate **BInt 7**; then, the intermediate **BInt 7** coordinated with one water molecule to produce complex **BCom 2**. Finally, the transition state **BTS 4** had an energy barrier of 12.52 kcal·mol⁻¹. The Nenitzescu target material **3h'** was then produced.

According to the joint experimental-computational results above, it can be concluded that (i) the rate-determining step for paths A and B is the formation of the C–N bond and the generation of enamine intermediate **BInt 3**, respectively; (ii) the origin of site-selectivity could be explained by following reasons: all energy barriers for the anti-Nenitzescu reaction can

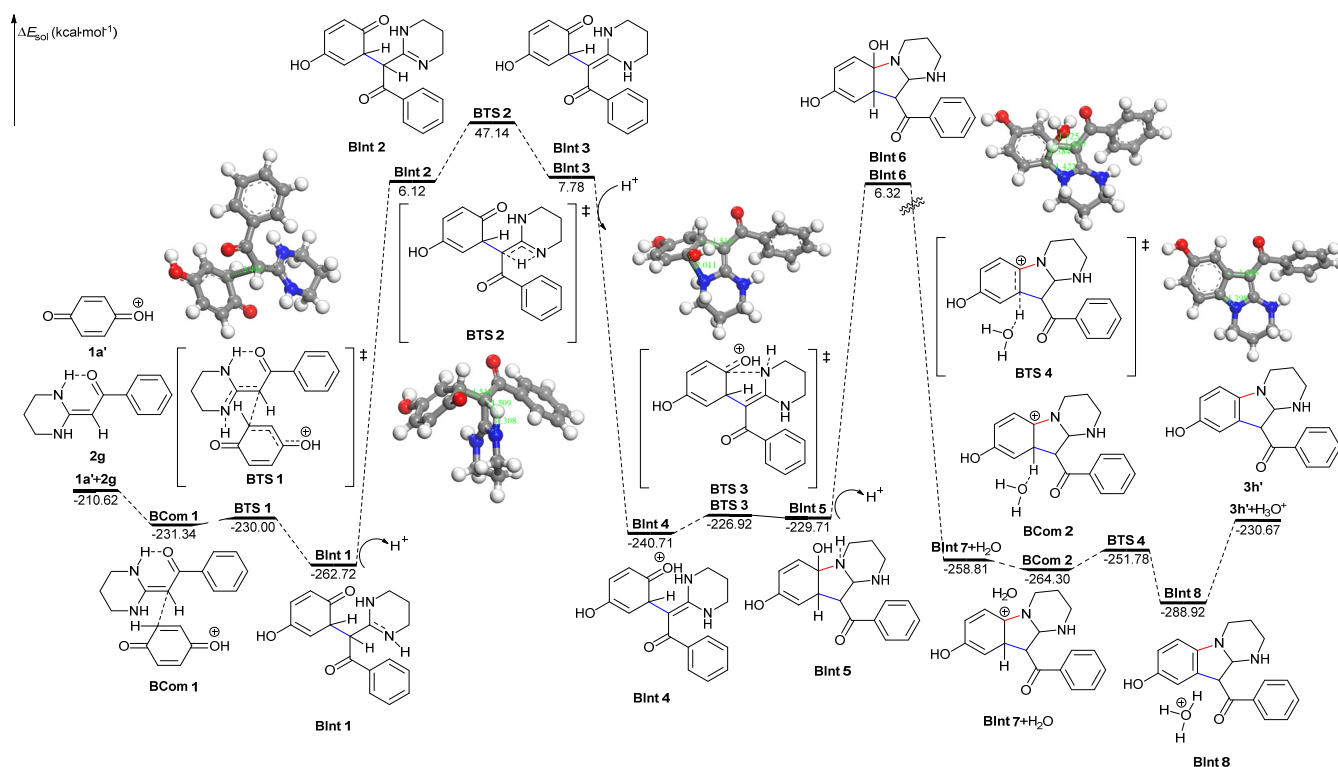


Fig. 5 Computed potential energy surface of the Nenitzescu reaction between **1a'** and **2g** at the m06/6-311+G(2d,2p)+ZPE[m06/6-31+G(d)] level. Relative energies (ΔE_{sol}), are with respect to **1a'+2g** and are given in kcal·mol⁻¹.

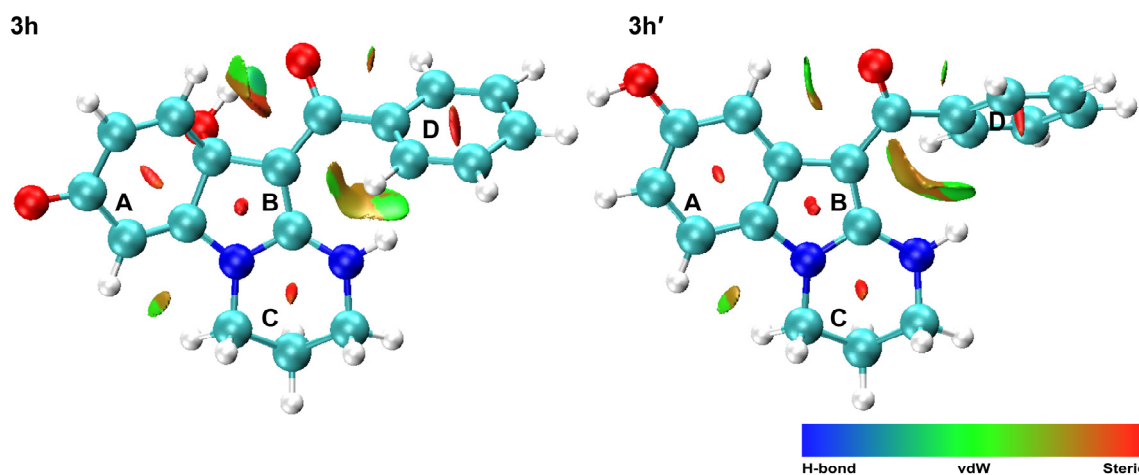


Fig. 6 Reduced density gradient isosurface of compounds **3h** and **3h'**. The color presented in the scale bar denotes the type of weak interaction (blue = hydrogen bond, green = van der Waals interaction, brown = weak steric effect, red = strong steric effect).

be overcome at ambient temperature, yet the extremely high energy barrier of imine-enamine tautomerization for the Nenitzescu reaction implies impossibility under the same conditions; (iii) the anti-Nenitzescu target material **3h** was produced rapidly (within 30 minutes) at room temperature, which implied that it is a kinetically stable compound; (iv) the Nenitzescu target material **3h'** was generated slowly (within 8 hours) and must be catalyzed by acetic acid at reflux temperature, which hinted that it is a thermodynamically stable

compound.

Of course, analysis of the types of changes in the weak interactions occurring here could provide valuable information to further explain the greater stability of the thermodynamically stable compound **3h'**. Therefore, we depicted the RDG isosurface²⁰ of the model compounds **3h** and **3h'** in Fig. 6. It can be observed that (i) whether for the kinetically stable **3h** or thermodynamically stable **3h'**, weak steric effects and van der Waals interactions among rings **A**, **B**, and **C** as well as **B**, **C**,

and **D** presented similar patterns; (ii) for **3h**, the hydroxyl donated a weak hydrogen bond (O—H···O) between rings **A** and **D** and the strong steric effect between rings **A** and **D** led to an increase in molecular energy; (iii) on the contrary, for **3h'**, only a few weak steric effects were found between rings **A** and **D**. As a result, the greater thermodynamic stability of **3h'** was mainly dependent on the release of the strong steric effect between rings **A** and **D**.

Conclusions

In conclusion, we have successfully developed the first site-selective methodology for the construction of a series of rarely fused [1,2-*a*]indolone derivatives **3** via an unexpected anti-Nenitzescu strategy. This modality displays remarkable virtues *viz.* it is environmentally benign, mild, rapid, and catalyst-free and has allowed us to prepare uncommon 3a-hydroxy-indol-6-one derivatives from a green perspective. In addition, it is promising that compounds **3** could transform into dehydroxylated indol-6-one **3i'** or aromatic 6-hydroxyindole **3i'** *in situ*. Importantly, with excellent solubility in water, ethanol, *etc.* the compound **3i'** may be of interest in medicinal chemistry because of its potential bioavailability. Our DFT computation results systematically elucidated the mechanistic details and controlling factors of the two Nenitzescu reactions. Therefore, we can anticipate that the theoretical investigation will yield valuable clues for finding the rate-determining steps and understanding the origin of the site-selectivity as well as providing answers to how this exceptional anti-Nenitzescu reaction actually occurs. Moreover, taking the experiment into cyberspace in order to avoid a futile waste of time and resources remains a unique aspect of green chemistry. Further studies aimed at exploring the *in vitro* biological activities and discovering related medicinal targets of compounds **3** are underway.

Experimental section

Computational methods

All calculations were carried out using the Gaussian 03 program.²¹ Geometry optimizations were performed with the M06 hybrid meta-GGA density functional^{18c} and the 6-31+G(d) basis set²² for the ground states and the transition states. The default self-consistent reaction field (SCRF) polarizable continuum model (PCM) was used with ethanol (dielectric constant $\epsilon = 24.852$) or 1,4-dioxane (dielectric constant $\epsilon = 2.2099$) as the solvent, while UFF radii were chosen as the atomic radii to define the molecular cavity. Vibrational frequencies were calculated for all stationary points to verify that each was a minimum (no imaginary frequencies) or a transition state (one imaginary frequency) on the potential energy surface and to achieve the relevant zero-point and thermal corrections to the electronic energies. Intrinsic reaction coordinate (IRC) calculations were also carried out to confirm the transition states connecting two relevant minima.²³ The

single-point energies and solvent effects were computed at the same level with the 6-311+G(2d,2p) basis set based on the previously optimized structures. The grid data for reduced density gradient (RDG) analysis was generated *via* the Multiwfn program²⁴ and visualized with VMD software.²⁵

General methods

All commercially available reagents were purchased from Adamas Reagent Co. Ltd. and used without further purification unless otherwise stated. Melting points were determined on a melting point apparatus and are uncorrected. ¹H (¹³C) NMR spectra were recorded at 500 (125) MHz using CDCl₃, DMSO-*d*₆, or their combination as the solvent. The chemical shifts (δ) are expressed in parts per million relative to the residual deuterated solvent signal, and coupling constants (*J*) are given in Hertz. HSQC, COSY, NOESY, and HMBC spectra were recorded on an NMR spectrometer at 500 MHz. IR spectra were recorded on an FT-IR-spectrometer using KBr pellets. HRMS data were obtained in electron impact (EI) mode at 70 eV. Intensities are reported as percentages relative to the base peak (*I* = 100%). The HPLC apparatus was equipped with a ZORBAX Original C₁₈ 7 μ m column (21.2 \times 250 mm).

Noncommercially available compounds

Synthesis of HKAs **2**. This series of compounds was prepared according to a procedure described in the literature.^{6a} The identity of the materials was confirmed by ¹H and ¹³C NMR, and by the MS spectra.

General procedure for the synthesis of compounds **3**

HKAs **2** (1.1 mmol) was added to a 50 mL round-bottomed flask and dissolved in ethanol (15 mL). An ethanolic solution (10 mL) of quinones **1** (1.0 mmol) was charged into a 25 mL dropping funnel and added slowly and dropwise over a period of 30 minutes. After all the ethanolic solution was added, a yellow precipitate formed. When the reaction completed as indicated by TLC, a small amount of H₂O (*ca.* 25 mL) was added and the mixture was extracted with EtOAc (50 mL \times 3). The combined organic extracts were dried over anhydrous Na₂SO₄ and evaporated *in vacuo*. The crude residue was dried and recrystallized from petroleum ether–EtOAc to afford the pure products **3**.

General procedure for the synthesis of compound **3i'**

Compound **3i** (1.0 mmol) and Et₃N (1.0 mmol) were added to 1,4-dioxane (30 mL) and the mixture was refluxed in a 50 mL round-bottomed flask. After **3i** was completely consumed (*ca.* 3 hours) as indicated by TLC, a deep purple solution formed. Then, the resulting solution was cooled to room temperature and diluted with a small amount of H₂O (*ca.* 20 mL). Afterward, the mixture was extracted with EtOAc (50 mL \times 3). The combined organic extracts were dried over anhydrous Na₂SO₄ and evaporated *in vacuo*. The crude residue was dried and recrystallized from petroleum ether–EtOAc to afford the pure product **3i'**.

General procedure for the synthesis of compound 3I'

Compound **3I** (1.0 mmol) and CH₃ONa (1.0 mmol) were added to methanol (25 mL) and the mixture was refluxed in a 50 mL round-bottomed flask. After **3I** was completely consumed (*ca.* 6 hours) as indicated by TLC, the resulting solution was cooled to room temperature and diluted with a small amount of H₂O (*ca.* 25 mL). Afterward, the mixture was extracted with EtOAc (50 mL × 3). The combined organic extracts were dried over anhydrous Na₂SO₄ and evaporated *in vacuo*. The pure product **3I'** was isolated by flash column chromatography of the residue obtained by evaporation of the filtrate on silica gel (200–300 mesh) with petroleum ether–EtOAc (1:1, v/v) as the eluent.²⁶

11a-Hydroxy-11-(4-methoxybenzoyl)-6-methyl-8,9,10,11a-tetrahydro-5H-benzo[e]imidazo[1,2-a]indol-5-one (3a). Purple solid, mp. 178–179 °C; IR (KBr) (ν_{\max} , cm⁻¹): 3418 (s), 3207 (m), 2964 (w), 1655 (s), 1588 (vs), 1524 (s), 1469 (m), 1399 (s), 1296 (s), 1245 (s), 1174 (m), 1100 (w), 1021 (w), 964 (w), 849 (w), 774 (w); ¹H NMR (500 MHz, DMSO-*d*₆) (δ , ppm): 9.80 (s, 1H, NH), 7.97 (d, *J* = 7.2 Hz, 1H, ArH), 7.83–7.73 (m, 3H, ArH), 7.14–7.12 (d, *J* = 8.4 Hz, 2H, ArH), 6.68–6.66 (d, *J* = 8.6 Hz, 2H, ArH), 3.68 (m, 2H, CH₂), 3.40 (m, 2H, CH₂), 3.61 (s, 3H, OCH₃), 1.99 (s, 3H, CH₃); ¹³C NMR (125 MHz, DMSO-*d*₆) (δ , ppm): 185.4 (d), 184.6, 163.8, 159.6, 145.4, 145.0, 136.9, 133.8, 133.7, 132.7, 132.4, 128.4, 126.4, 125.8, 113.0, 83.8, 60.1, 55.3, 43.9, 42.2, 15.1; HRMS (ESI-TOF, [M]⁺): calcd for C₂₃H₂₀N₂O₄, 388.1418; found, 388.1391.

11a-Hydroxy-6-methyl-11-(4-methylbenzoyl)-8,9,10,11a-tetrahydro-5H-benzo[e]imidazo[1,2-a]indol-5-one (3b). Purple solid, mp. 180–181 °C; IR (KBr) (ν_{\max} , cm⁻¹): 3408 (s), 3070 (w), 2960 (w), 2881 (w), 1655 (s), 1590 (vs), 1528 (s), 1480 (m), 1399 (m), 1295 (s), 1182 (w), 1170 (w), 1037 (w), 955 (w), 841 (w), 758 (m); ¹H NMR (500 MHz, CDCl₃) (δ , ppm): 10.0 (s, 1H, NH), 7.81 (d, *J* = 6.2 Hz, 1H, ArH), 7.75 (d, *J* = 6.2 Hz, 1H, ArH), 7.50–7.49 (m, 2H, ArH), 7.05 (d, *J* = 7.6 Hz, 2H, ArH), 6.84 (d, *J* = 7.6 Hz, 2H, ArH), 5.56 (s, 1H, OH), 3.77 (m, 2H, CH₂), 3.50 (m, 2H, CH₂), 2.15 (s, 3H, CH₃), 1.97 (s, 3H, CH₃); ¹³C NMR (125 MHz, CDCl₃) (δ , ppm): 188.8, 185.8 (d), 164.6, 145.8, 145.5, 140.8, 139.1, 133.4, 132.8, 132.4, 128.6, 127.2, 126.7, 126.2, 85.2, 44.2, 42.9, 21.6, 15.4; HRMS (ESI-TOF, [M]⁺): calcd for C₂₃H₂₀N₂O₃, 372.1468; found, 372.1437.

11-(4-Chlorobenzoyl)-11a-hydroxy-6-methyl-8,9,10,11a-tetrahydro-5H-benzo[e]imidazo[1,2-a]indol-5-one (3c). Purple solid, mp. 181–182 °C; IR (KBr) (ν_{\max} , cm⁻¹): 3423 (s), 3215 (s), 2939 (w), 2883 (w), 1655 (s), 1592 (vs), 1527 (s), 1486 (m), 1402 (m), 1297 (s), 1174 (w), 1084 (w), 998 (w), 958 (w), 833 (w), 762 (w); ¹H NMR (500 MHz, DMSO-*d*₆) (δ , ppm): 9.74 (s, 1H, NH), 7.97 (d, *J* = 7.3 Hz, 1H, ArH), 7.81–7.73 (m, 3H, ArH), 7.20–7.14 (m, 4H, ArH), 3.70 (m, 2H, CH₂), 3.40 (m, 2H, CH₂), 2.01 (s, 3H, CH₃); ¹³C NMR (125 MHz, DMSO-*d*₆) (δ , ppm): 185.3, 184.4, 163.7, 145.7, 144.6, 143.1, 142.0, 133.8, 133.0, 132.5, 132.4, 128.6, 127.8, 126.3, 125.8, 83.9, 44.0, 42.2, 15.2; HRMS (ESI-TOF, [M]⁺): calcd for C₂₂H₁₇ClN₂O₃, 392.0922; found, 392.0894.

12b-Hydroxy-13-(4-methylbenzoyl)-1,2,3,12b-tetrahydro-6H-imidazo[1,2-a]naphtho[2,3-e]indol-6-one (3d). Yellow solid, mp. 158–159 °C; IR (KBr) (ν_{\max} , cm⁻¹): 3423 (s), 3226 (w), 3070 (w), 2964 (w), 2862 (w), 1679 (s), 1569 (vs), 1512 (vs), 1472 (w), 1386 (m), 1335 (w), 1275 (m), 1161 (m), 1072 (w), 989 (w), 908 (w), 841 (w), 754 (w); ¹H NMR (500 MHz, DMSO-*d*₆) (δ , ppm): 9.10 (s, 1H, NH), 8.54 (s, 1H, ArH), 8.20 (s, 1H, ArH), 8.11–8.09 (m, 2H, ArH), 7.69–7.66 (m, 1H, ArH), 7.61–7.58 (m, 1H, ArH), 7.34 (d, *J* = 7.6 Hz, 2H, ArH), 7.22 (d, *J* = 7.7 Hz, 2H, ArH), 7.12 (s, 1H, ArH), 3.95 (s, 1H, CH), 3.80–3.78 (m, 1H, CH₂), 3.48–3.45 (m, 3H, CH₂), 2.37 (s, 1H, CH₃); ¹³C NMR (125 MHz, DMSO-*d*₆) (δ , ppm): 194.7, 188.6, 159.6, 140.7, 137.9, 137.6, 134.9, 132.0, 129.8, 129.2, 128.6, 128.2, 127.4, 123.7, 81.8, 79.0, 43.5, 42.0, 41.7, 21.30; HRMS (ESI-TOF, [M + H]⁺): calcd for C₂₆H₂₁N₂O₃, 409.1547; found, 409.1557.

13-Benzoyl-12b-hydroxy-1,2,3,12b-tetrahydro-6H-imidazo[1,2-a]naphtho[2,3-e]indol-6-one (3e). Yellow solid, mp. 292–293 °C; IR (KBr) (ν_{\max} , cm⁻¹): 3408 (s), 2913 (w), 1657 (w), 1582 (vs), 1453 (w), 1398 (m), 1331 (w), 1271 (m), 1162 (w), 1053 (w), 995 (w), 919 (w), 762 (w); ¹H NMR (500 MHz, DMSO-*d*₆) (δ , ppm): 9.15 (s, 1H, NH), 8.40 (s, 1H, ArH), 8.12–8.06 (m, 4H, ArH), 7.65–7.49 (m, 5H, ArH), 7.42 (s, 1H, ArH), 5.33 (s, 1H, CH), 4.33 (m, 1H, CH₂), 3.98–3.92 (m, 2H, CH₂), 3.62 (m, 1H, CH₂); ¹³C NMR (125 MHz, DMSO-*d*₆) (δ , ppm): 187.3, 182.4, 166.7, 141.6, 136.9, 134.5, 134.0, 132.4, 130.7, 130.3, 130.0, 129.7, 128.7, 128.5, 127.9, 127.5, 123.6, 109.5, 91.8, 85.7, 43.3, 42.2; HRMS (ESI-TOF, [M]⁺): calcd for C₂₅H₁₈N₂O₃, 394.1312; found, 394.1274.

13-(4-Chlorobenzoyl)-12b-hydroxy-1,2,3,12b-tetrahydro-6H-imidazo[1,2-a]naphtho[2,3-e]indol-6-one (3f). Yellow solid, mp. 250–251 °C; IR (KBr) (ν_{\max} , cm⁻¹): 3455 (s), 3054 (w), 2968 (w), 2885 (w), 1656 (s), 1578 (vs), 1531 (s), 1488 (w), 1386 (m), 1312 (w), 1273 (m), 1076 (w), 1010 (w), 962 (w), 908 (w), 825 (w), 758 (w); ¹H NMR (500 MHz, DMSO-*d*₆) (δ , ppm): 9.09 (s, 1H, NH), 8.41 (s, 1H, ArH), 8.12–8.06 (m, 4H, ArH), 7.65–7.59 (m, 5H, ArH), 7.43 (s, 1H, ArH), 5.43 (s, 1H, CH), 4.33 (m, 1H, CH₂), 4.04–4.03 (m, 2H, CH₂), 3.62 (m, 1H, CH₂); ¹³C NMR (125 MHz, DMSO-*d*₆) (δ , ppm): 185.7, 182.6, 166.5, 140.2, 136.8, 135.4, 134.0, 132.4, 130.3, 129.7, 129.5, 129.3, 128.9, 128.5, 128.4, 128.0, 127.5, 127.4, 123.6, 109.7, 91.7, 85.7, 43.3, 42.1; HRMS (ESI-TOF, [M]⁺): calcd for C₂₅H₁₇ClN₂O₃, 428.0922; found, 428.0884.

9a-Hydroxy-10-(4-methylbenzoyl)-1,3,4,9a-tetrahydro-pyrimido[1,2-a]indol-7(2H)-one (3g). Yellow solid, mp. 148–149 °C; IR (KBr) (ν_{\max} , cm⁻¹): 3416 (s), 2968 (w), 2866 (w), 1641 (s), 1557 (vs), 1531 (vs), 1416 (m), 1357 (w), 1316 (w), 1253 (m), 1170 (w), 1080 (w), 1025 (w), 923 (w), 837 (w), 754 (w); ¹H NMR (500 MHz, DMSO-*d*₆) (δ , ppm): 9.46 (s, 1H, NH), 7.44 (d, 2H, *J* = 7.9 Hz, ArH), 7.26 (d, 2H, *J* = 7.8 Hz, ArH), 7.12 (s, 1H, ArH), 7.03 (d, 1H, ArH), 5.84–5.81 (m, 1H, CH₂), 4.80 (s, 1H, CH), 3.42 (m, 2H, CH₂), 2.40 (s, 1H, CH₂), 2.37 (s, 3H, CH₃), 2.00–1.94 (m, 2H, CH₂); ¹³C NMR (125 MHz, DMSO-*d*₆) (δ , ppm): 187.1, 184.4, 162.9, 162.0, 140.2, 139.0, 137.6, 129.8, 129.1, 127.6, 106.8, 93.3, 85.5, 38.4, 36.3, 21.4, 20.1; HRMS (ESI-TOF, [M]⁺): calcd for C₁₉H₁₈N₂O₃,

322.1312; found, 322.1276.

10-Benzoyl-9a-hydroxy-1,3,4,9a-tetrahydropyrimido[1,2-*a*]indol-7(2*H*)-one (3h). Purple solid, mp. 149–150 °C; IR (KBr) (ν_{\max} , cm^{-1}): 3416 (s), 3317 (w), 2970 (w), 2874 (w), 1642 (s), 1555 (vs), 1522 (vs), 1417 (m), 1358 (w), 1321 (w), 1253 (m), 1166 (w), 1072 (w), 1017 (w), 931 (w), 895 (w), 856 (w), 790 (w), 754 (w); ^1H NMR (500 MHz, DMSO-*d*₆) (δ , ppm): 9.47 (s, 1H, NH), 7.51–7.45 (m, 5H, ArH), 7.13 (s, 1H, ArH), 7.05–7.02 (m, 1H, ArH), 5.84–5.82 (m, 1H, CH₂), 4.69 (s, 1H, CH), 3.43–3.41 (m, 3H, CH₂), 2.00–1.95 (m, 2H, CH₂); ^{13}C NMR (125 MHz, DMSO-*d*₆) (δ , ppm): 187.2, 184.4, 162.8, 161.8, 141.9, 137.6, 130.4, 129.8, 128.6, 127.4, 106.9, 93.3, 85.5, 38.4, 36.3, 20.1; HRMS (ESI-TOF, [M]⁺): calcd for C₁₈H₁₆N₂O₃, 308.1155; found, 308.1129.

12a-Hydroxy-12-(4-methoxybenzoyl)-9,10,11,12a-tetrahydrobenzo[*e*]pyrimido[1,2-*a*]indol-5(8*H*)-one (3i). Yellow solid, mp. 160–162 °C; IR (KBr) (ν_{\max} , cm^{-1}): 3726 (s), 3282 (m), 2962 (w), 2880 (w), 1603 (s), 1547 (vs), 1506 (vs), 1412 (w), 1329 (m), 1258 (s), 1172 (w), 1127 (w), 1022 (w), 942 (w), 842 (w), 774 (w); ^1H NMR (500 MHz, DMSO-*d*₆) (δ , ppm): 9.61 (s, 1H, NH), 7.81 (d, *J* = 7.2 Hz, 1H, ArH), 7.71 (d, *J* = 7.2 Hz, 1H, ArH), 7.57 (d, *J* = 7.9 Hz, 2H, ArH), 7.47–7.39 (m, 2H, ArH), 7.04 (s, 1H, ArH), 7.03 (s, 1H, ArH), 5.10 (s, 1H, CH), 4.14–4.12 (m, 1H, CH₂), 3.84 (s, 3H, CH₃), 3.60 (m, 1H, CH₂), 3.37–3.32 (m, 2H, CH₂), 2.17–2.13 (m, 1H, CH₂), 1.80 (m, 1H, CH₂); ^{13}C NMR (125 MHz, DMSO-*d*₆) (δ , ppm): 187.6, 182.1, 162.8, 161.3, 140.8, 134.2, 132.8, 130.9, 129.6, 128.6, 126.6, 124.0, 113.9, 105.8, 93.5, 88.5, 55.6, 41.0, 38.5, 21.4; HRMS (ESI-TOF, [M + H]⁺): calcd for C₂₃H₂₁N₂O₄, 389.1496; found, 389.1476.

12a-Hydroxy-12-(4-methylbenzoyl)-9,10,11,12a-tetrahydrobenzo[*e*]pyrimido[1,2-*a*]indol-5(8*H*)-one (3j). Yellow solid, mp. 175–176 °C; IR (KBr) (ν_{\max} , cm^{-1}): 3462 (s), 3253 (w), 1601 (s), 1549 (vs), 1503 (vs), 1413 (w), 1328 (m), 1261 (s), 1123 (m), 1029 (w), 939 (w), 845 (w), 772 (w); ^1H NMR (500 MHz, DMSO-*d*₆) (δ , ppm): 9.63 (s, 1H, NH), 7.78 (d, *J* = 7.1 Hz, 1H, ArH), 7.70 (d, *J* = 7.2 Hz, 1H, ArH), 7.48–7.42 (m, 4H, ArH), 7.03 (d, *J* = 7.8 Hz, 2H, ArH), 4.98 (s, 1H, CH), 4.14–4.11 (m, 1H, CH₂), 3.87–3.83 (m, 1H, CH₂), 3.61 (m, 1H, CH₂), 2.40 (m, 3H, CH₃), 2.20–2.17 (m, 1H, CH₂), 1.78 (m, 2H, CH₂); ^{13}C NMR (125 MHz, DMSO-*d*₆) (δ , ppm): 188.2, 182.2, 162.6, 140.8, 140.2, 139.2, 132.8, 130.9, 129.2, 128.6, 127.5, 126.6, 123.9, 106.0, 93.5, 88.5, 41.0, 38.5, 21.4, 21.3; HRMS (ESI-TOF, [M + H]⁺): calcd for C₂₃H₂₁N₂O₃, 373.1547; found, 373.1540.

12-Benzoyl-12a-hydroxy-9,10,11,12a-tetrahydrobenzo[*e*]pyrimido[1,2-*a*]indol-5(8*H*)-one (3k). Yellow solid, mp. 165–166 °C; IR (KBr) (ν_{\max} , cm^{-1}): 3271 (s), 3061 (w), 2960 (w), 1601 (s), 1568 (vs), 1515 (vs), 1413 (w), 1323 (m), 1268 (s), 1130 (w), 1088 (w), 1033 (w), 984 (w), 812 (w), 749 (w); ^1H NMR (500 MHz, DMSO-*d*₆) (δ , ppm): 9.66 (s, 1H, NH), 7.79 (d, *J* = 7.2 Hz, 1H, ArH), 7.70 (d, *J* = 7.4 Hz, 1H, ArH), 7.52–7.40 (m, 7H, ArH), 4.88 (s, 1H, CH), 4.14–4.12 (m, 1H, CH₂), 3.87–3.83 (m, 1H, CH₂), 3.62 (m, 1H, CH₂), 3.37–3.28 (m, 1H, CH₂), 2.19–2.17 (m, 1H, CH₂), 1.80 (m, 1H, CH₂); ^{13}C NMR (125 MHz, DMSO-*d*₆) (δ , ppm): 188.8, 182.9, 163.2,

163.0, 142.6, 141.3, 133.3, 131.4, 130.8, 129.2, 129.1, 127.7, 127.1, 124.4, 106.6, 94.0, 89.1, 41.5, 39.0, 21.8; HRMS (ESI-TOF, [M + H]⁺): calcd for C₂₂H₁₉N₂O₃, 359.1390; found, 359.1380.

12-(4-Chlorobenzoyl)-12a-hydroxy-9,10,11,12a-tetrahydrobenzo[*e*]pyrimido[1,2-*a*]indol-5(8*H*)-one (3l). Yellow solid, mp. 168–169 °C; IR (KBr) (ν_{\max} , cm^{-1}): 3280 (s), 2974 (w), 2875 (w), 1598 (s), 1550 (vs), 1507 (w), 1415 (w), 1323 (m), 1258 (s), 1123 (w), 1087 (w), 1014 (w), 939 (w), 904 (w), 825 (w), 770 (w), 706 (w); ^1H NMR (500 MHz, DMSO-*d*₆) (δ , ppm): 9.61 (s, 1H, NH), 7.84 (d, *J* = 7.6 Hz, 1H, ArH), 7.71 (d, *J* = 7.6 Hz, 1H, ArH), 7.60–7.52 (m, 4H, ArH), 7.49–7.41 (m, 2H, ArH), 4.90 (s, 1H, CH), 4.14–4.12 (m, 1H, CH₂), 3.88–3.83 (m, 1H, CH₂), 3.64–3.61 (m, 1H, CH₂), 3.35–3.33 (m, 1H, CH₂), 2.20–2.18 (m, 1H, CH₂), 1.80–1.77 (m, 1H, CH₂); ^{13}C NMR (125 MHz, DMSO-*d*₆) (δ , ppm): 186.6, 182.4, 162.6, 162.2, 140.7, 135.0, 132.7, 131.0, 129.4, 128.9, 128.6, 126.6, 124.0, 106.3, 93.4, 88.6, 41.0, 38.6, 21.3; HRMS (ESI-TOF, [M + H]⁺): calcd for C₂₂H₁₈ClN₂O₃, 393.1000; found, 393.0990.

12-Benzoyl-12a-hydroxy-6-methyl-9,10,11,12a-tetrahydrobenzo[*e*]pyrimido[1,2-*a*]indol-5(8*H*)-one (3m). Purple solid, mp. 186–187 °C; IR (KBr) (ν_{\max} , cm^{-1}): 3426 (s), 2956 (w), 2878 (w), 1654 (s), 1593 (vs), 1528 (s), 1476 (w), 1401 (w), 1296 (s), 1182 (w), 1053 (w), 1018 (w), 951 (w), 833 (w), 754 (w); ^1H NMR (500 MHz, DMSO-*d*₆) (δ , ppm): 9.80 (s, 1H, NH), 7.96 (d, *J* = 6.9 Hz, 1H, ArH), 7.82 (d, *J* = 6.8 Hz, 1H, ArH), 7.78–7.74 (m, 2H, ArH), 7.05 (d, *J* = 7.4 Hz, 3H, ArH), 6.92 (d, *J* = 7.2 Hz, 2H, ArH), 4.14 (m, 1H, CH₂), 3.69 (m, 3H, CH₂), 2.36 (m, 1H, CH₂), 2.14 (s, 3H, CH₃), 1.36 (m, 1H, CH₂); ^{13}C NMR (125 MHz, DMSO-*d*₆) (δ , ppm): 185.6 (d), 184.5, 163.8, 145.2, 141.6, 137.9, 133.8, 133.7, 132.6, 132.4, 128.6, 128.2, 127.3, 126.8, 126.4, 125.8, 83.9, 44.0, 42.2, 21.1; HRMS (ESI-TOF, [M]⁺): calcd for C₂₃H₂₀N₂O₃, 372.1468; found, 372.1438.

13b-Hydroxy-14-(4-methylbenzoyl)-1,3,4,13b-tetrahydro-naphtho[2,3-*e*]pyrimido[1,2-*a*]indol-7(2*H*)-one (3n). Yellow solid, mp. 173–174 °C; IR (KBr) (ν_{\max} , cm^{-1}): 3419 (s), 3266 (w), 2924 (w), 2864 (w), 1584 (vs), 1505 (w), 1443 (w), 1406 (w), 1327 (w), 1257 (m), 1187 (m), 1100 (w), 1033 (w), 990 (w), 821 (w), 747 (w); ^1H NMR (500 MHz, DMSO-*d*₆) (δ , ppm): 9.62 (s, 1H, NH), 8.33 (s, 1H, ArH), 8.14 (s, 1H, ArH), 8.05–8.02 (m, 1H, ArH), 7.61 (d, *J* = 7.4 Hz, 1H, ArH), 7.57–7.54 (m, 2H, ArH), 7.44 (d, *J* = 8.0 Hz, 2H, ArH), 7.30 (d, *J* = 7.2 Hz, 1H, ArH), 7.14 (d, *J* = 7.4 Hz, 1H, ArH), 5.05 (s, 1H, CH), 4.21 (m, 1H, CH₂), 4.11 (m, 1H, CH₂), 3.66 (m, 1H, CH₂), 2.40 (s, 3H, CH₃), 2.09 (m, 1H, CH₂), 1.83 (m, 2H, CH₂); ^{13}C NMR (125 MHz, DMSO-*d*₆) (δ , ppm): 188.5, 182.4, 162.6, 162.3, 160.0, 140.2, 139.8, 139.3, 133.4, 132.3, 131.2, 129.4, 129.2, 128.7, 128.6, 128.3, 127.5, 122.6, 106.6, 93.4, 89.0, 76.7, 41.0, 38.7, 37.8, 21.4; HRMS (ESI-TOF, [M]⁺): calcd for C₂₇H₂₂N₂O₃, 422.1625; found, 422.1586.

13a-Hydroxy-13-(4-methoxybenzoyl)-8,9,10,11,12,13a-hexahydro-5*H*-benzo[*e*][1,3]diazepino[1,2-*a*]indol-5-one (3o). Yellow solid, mp. 184–185 °C; IR (KBr) (ν_{\max} , cm^{-1}): 3423 (s), 2944 (w), 2842 (w), 1598 (vs), 1551 (m), 1506 (w),

1449 (w), 1410 (w), 1369 (w), 1250 (s), 1174 (w), 1115 (w), 1084 (w), 1010 (w), 928 (w), 879 (w), 833 (w), 786 (w); ^1H NMR (500 MHz, DMSO- d_6) (δ , ppm): 10.1 (s, 1H, NH), 7.76 (d, $J = 6.4$ Hz, 1H, ArH), 7.56 (d, $J = 7.0$ Hz, 2H, ArH), 7.50–7.48 (m, 2H, ArH), 7.41 (s, 1H, ArH), 7.04 (d, $J = 7.2$ Hz, 2H, ArH), 4.98 (s, 1H, CH), 4.16–4.13 (m, 1H, CH $_2$), 3.84 (s, 3H, CH $_3$), 3.75 (m, 1H, CH $_2$), 3.53–3.48 (m, 2H, CH $_2$), 2.09 (m, 1H, CH $_2$), 1.99 (m, 2H, CH $_2$), 1.76 (m, 1H, CH $_2$); ^{13}C NMR (125 MHz, DMSO- d_6) (δ , ppm): 188.6, 182.7, 171.1, 162.4, 161.4, 141.5, 134.0, 133.0, 131.0, 129.6, 128.6, 126.6, 123.3, 113.9, 105.6, 94.7, 89.4, 55.7, 46.3, 43.9, 26.6, 26.3; HRMS (ESI-TOF, $[\text{M}]^+$): calcd for C $_{24}$ H $_{22}$ N $_2$ O $_4$, 402.1574; found, 402.1530.

13a-Hydroxy-13-(4-methylbenzoyl)-8,9,10,11,12,13a-hexahydro-5H-benzo[e][1,3]diazepino[1,2-a]indol-5-one (3p). Yellow solid, mp. 179–180 °C; IR (KBr) (ν_{max} , cm $^{-1}$): 3403 (s), 3223 (w), 2924 (w), 2862 (w), 1599 (vs), 1554 (m), 1510 (w), 1454 (w), 1373 (m), 1329 (w), 1259 (s), 1170 (w), 1119 (w), 1084 (w), 1014 (w), 984 (w), 829 (w), 774 (w); ^1H NMR (500 MHz, DMSO- d_6) (δ , ppm): 10.16 (s, 1H, NH), 7.75 (d, $J = 7.2$ Hz, 1H, ArH), 7.48–7.40 (m, 5H, ArH), 7.29 (d, $J = 7.1$ Hz, 2H, ArH), 4.89 (s, 1H, CH), 4.16–4.14 (m, 1H, CH $_2$), 3.76 (m, 1H, CH $_2$), 3.58–3.47 (m, 2H, CH $_2$), 2.40 (s, 3H, CH $_3$), 2.12 (m, 1H, CH $_2$), 2.01 (m, 2H, CH $_2$), 1.79 (m, 1H, CH $_2$); ^{13}C NMR (125 MHz, DMSO- d_6) (δ , ppm): 189.2, 182.8, 171.0, 162.3, 141.5, 140.4, 139.1, 133.0, 130.9, 129.2, 128.6, 127.5, 126.6, 123.3, 105.8, 94.7, 89.6, 46.2, 43.9, 26.6, 26.3, 21.5; HRMS (ESI-TOF, $[\text{M}]^+$): calcd for C $_{24}$ H $_{22}$ N $_2$ O $_3$, 386.1625; found, 386.1599.

13-Benzoyl-13a-hydroxy-8,9,10,11,12,13a-hexahydro-5H-benzo[e][1,3]diazepino[1,2-a]indol-5-one (3q). Yellow solid, mp. 188–189 °C; IR (KBr) (ν_{max} , cm $^{-1}$): 3440 (s), 3146 (w), 2921 (w), 2864 (w), 1605 (s), 1552 (vs), 1516 (m), 1454 (w), 1377 (m), 1323 (w), 1254 (s), 1127 (w), 1082 (w), 1005 (w), 984 (w), 800 (w), 764 (w); ^1H NMR (500 MHz, DMSO- d_6) (δ , ppm): 10.18 (s, 1H, NH), 7.74 (d, $J = 7.2$ Hz, 1H, ArH), 7.51–7.49 (m, 7H, ArH), 7.41 (s, 1H, ArH), 4.75 (s, 1H, CH), 4.16–4.14 (m, 1H, CH $_2$), 3.78 (m, 1H, CH $_2$), 3.58–3.52 (m, 2H, CH $_2$), 2.11 (m, 1H, CH $_2$), 2.01–2.00 (m, 2H, CH $_2$), 1.80 (m, 1H, CH $_2$); ^{13}C NMR (125 MHz, DMSO- d_6) (δ , ppm): 189.2, 182.9, 162.1, 142.0, 141.5, 133.0, 131.0, 130.4, 128.8, 128.6, 127.1, 126.6, 125.9, 123.2, 106.0, 94.6, 89.6, 46.2, 43.9, 26.6, 26.3; HRMS (ESI-TOF, $[\text{M}]^+$): calcd for C $_{23}$ H $_{20}$ N $_2$ O $_3$, 372.1468; found, 372.1437.

13-(4-Chlorobenzoyl)-13a-hydroxy-8,9,10,11,12,13a-hexahydro-5H-benzo[e][1,3]diazepino[1,2-a]indol-5-one (3r). Yellow solid, mp. 160–161 °C; IR (KBr) (ν_{max} , cm $^{-1}$): 3521 (m), 3348 (s), 3233 (w), 2964 (w), 1601 (s), 1553 (vs), 1502 (s), 1409 (m), 1324 (w), 1256 (s), 1174 (w), 1123 (w), 1088 (w), 1049 (w), 1010 (w), 912 (w), 829 (w), 778 (w); ^1H NMR (500 MHz, DMSO- d_6) (δ , ppm): 10.10 (s, 1H, NH), 7.75 (d, $J = 7.4$ Hz, 1H, ArH), 7.59–7.49 (m, 6H, ArH), 7.43 (d, $J = 8.1$ Hz, 1H, ArH), 4.79 (s, 1H, CH), 4.14 (m, 1H, CH $_2$), 3.77 (m, 1H, CH $_2$), 3.60–3.50 (m, 2H, CH $_2$), 2.10–2.01 (m, 2H, CH $_2$), 1.80 (m, 1H, CH $_2$); ^{13}C NMR (125 MHz, DMSO- d_6) (δ , ppm): 187.6, 183.0, 170.7, 161.9, 141.4, 140.5, 135.2, 132.8,

131.1, 129.3, 129.0, 128.7, 126.7, 123.3, 106.0, 94.5, 89.6, 46.2, 43.9, 26.5, 26.2; HRMS (ESI-TOF, $[\text{M}]^+$): calcd for C $_{23}$ H $_{19}$ ClN $_2$ O $_3$, 406.1079; found, 406.1039.

14b-Hydroxy-15-(4-methylbenzoyl)-1,2,3,4,5,14b-hexahydro-8H-[1,3]diazepino[1,2-a]naphtho[2,3-e]indol-8-one (3s). Yellow solid, mp. 221–222 °C; IR (KBr) (ν_{max} , cm $^{-1}$): 3425 (s), 3066 (w), 2968 (w), 2921 (w), 2858 (w), 1580 (vs), 1505 (w), 1449 (w), 1376 (w), 1331 (w), 1262 (m), 1178 (w), 1100 (w), 1053 (w), 1006 (w), 904 (w), 829 (w), 758 (w); ^1H NMR (500 MHz, DMSO- d_6) (δ , ppm): 10.17 (s, 1H, NH), 8.31 (s, 1H, ArH), 8.03 (d, $J = 7.8$ Hz, 2H, ArH), 7.89 (s, 1H, ArH), 7.63 (t, $J = 7.4$ Hz, 1H, ArH), 7.58–7.54 (m, 1H, ArH), 7.44 (d, $J = 7.2$ Hz, 2H, ArH), 7.31 (d, $J = 7.2$ Hz, 2H, ArH), 4.96 (s, 1H, CH), 4.39–4.29 (m, 2H, CH $_2$), 3.81–3.79 (m, 1H, CH $_2$), 3.67–3.58 (m, 3H, CH $_2$), 2.41 (s, 3H, CH $_3$), 2.03 (m, 1H, CH $_2$), 1.85 (m, 1H, CH $_2$); ^{13}C NMR (125 MHz, DMSO- d_6) (δ , ppm): 189.4, 182.8, 170.4, 161.8, 140.9, 140.4, 139.1, 137.2, 133.3, 132.4, 131.3, 129.5, 129.2, 128.6, 128.4, 127.4, 122.2, 106.6, 94.4, 89.9, 56.4, 46.0, 43.7, 26.7, 26.4, 21.4; HRMS (ESI-TOF, $[\text{M}]^+$): calcd for C $_{28}$ H $_{24}$ N $_2$ O $_3$, 436.1781; found, 436.1742.

15-Benzoyl-14b-hydroxy-1,2,3,4,5,14b-hexahydro-8H-[1,3]diazepino[1,2-a]naphtho[2,3-e]indol-8-one (3t). Yellow solid, mp. 222–223 °C; IR (KBr) (ν_{max} , cm $^{-1}$): 3415 (s), 3192 (w), 3058 (w), 2917 (w), 2850 (w), 1586 (s), 1557 (vs), 1511 (s), 1446 (m), 1378 (m), 1331 (w), 1256 (m), 1194 (w), 1108 (w), 1049 (w), 1002 (w), 888 (w), 821 (w), 790 (w), 747 (w); ^1H NMR (500 MHz, DMSO- d_6) (δ , ppm): 10.19 (s, 1H, NH), 8.31 (s, 1H, ArH), 8.03 (d, $J = 7.6$ Hz, 2H, ArH), 7.90 (s, 1H, ArH), 7.64–7.61 (m, 2H, ArH), 7.57–7.52 (m, 5H, ArH), 4.84 (s, 1H, CH), 4.33–4.30 (m, 1H, CH $_2$), 3.88 (m, 2H, CH $_2$), 3.81–3.79 (m, 2H, CH $_2$), 2.03 (m, 2H, CH $_2$), 1.86 (m, 1H, CH $_2$); ^{13}C NMR (125 MHz, DMSO- d_6) (δ , ppm): 189.4, 182.9, 170.4, 161.7, 142.0, 137.1, 133.7, 133.3, 132.4, 131.3, 130.5, 129.5, 128.8, 128.6, 128.5, 127.6, 127.4, 127.1, 122.2, 106.8, 94.4, 90.0, 46.0, 43.7, 26.7, 26.4; HRMS (ESI-TOF, $[\text{M}]^+$): calcd for C $_{27}$ H $_{22}$ N $_2$ O $_3$, 422.1625; found, 422.1593.

15-(4-Chlorobenzoyl)-14b-hydroxy-1,2,3,4,5,14b-hexahydro-8H-[1,3]diazepino[1,2-a]naphtho[2,3-e]indol-8-one (3u). Yellow solid, mp. 228–229 °C; IR (KBr) (ν_{max} , cm $^{-1}$): 3426 (s), 2972 (w), 2913 (w), 1632 (w), 1583 (vs), 1512 (w), 1441 (w), 1376 (w), 1335 (w), 1257 (m), 1190 (w), 1096 (w), 1053 (w), 1009 (w), 904 (w), 829 (w), 762 (w); ^1H NMR (500 MHz, DMSO- d_6) (δ , ppm): 10.12 (s, 1H, NH), 8.33 (s, 1H, ArH), 8.04 (d, $J = 8.1$ Hz, 2H, ArH), 7.91 (s, 1H, ArH), 7.64–7.55 (m, 6H, ArH), 4.88 (s, 1H, CH), 4.34–4.31 (m, 1H, CH $_2$), 3.82–3.79 (m, 1H, CH $_2$), 3.71–3.60 (m, 3H, CH $_2$), 2.02 (m, 2H, CH $_2$), 1.86 (m, 1H, CH $_2$); ^{13}C NMR (125 MHz, DMSO- d_6) (δ , ppm): 187.8, 182.9, 170.2, 161.4, 140.6, 137.0, 135.2, 133.4, 132.4, 131.1, 129.6, 129.3, 129.0, 128.6, 127.6, 127.5, 122.2, 106.8, 94.4, 90.0, 45.9, 43.7, 26.6, 26.3; HRMS (ESI-TOF, $[\text{M}]^+$): calcd for C $_{27}$ H $_{21}$ ClN $_2$ O $_3$, 456.1235; found, 456.1197.

(5,11a-Dihydroxy-6-methyl-9,11a-dihydro-10H-benzo[g]-imidazo[1,2-a]indol-7-yl)(*p*-tolyl)methanone (3b'). Purple solid, mp. 165–166 °C; IR (KBr) (ν_{max} , cm $^{-1}$): 3414 (s), 2925 (m), 2882 (w), 1592 (vs), 1528 (w), 1403 (m), 1283 (w), 1166

(w), 1080 (w), 1024 (w), 954 (w), 841 (w), 755 (w); ^1H NMR (500 MHz, DMSO- d_6) 8.30 (s, 1H, OH), 8.03–7.96 (m, 2H, ArH), 7.84 (m, 2H, ArH), 7.68 (m, 2H, ArH), 7.21 (m, 2H, ArH), 3.55 (m, 2H, CH₂), 3.24 (m, 2H, CH₂), 2.34 (s, 3H, CH₃), 2.08 (s, 3H, CH₃); ^{13}C NMR (125 MHz, DMSO- d_6) (δ , ppm): 184.8, 184.1, 168.7, 166.8, 145.6, 141.3, 141.2, 134.2, 132.1, 131.8, 129.1, 127.5, 126.3, 39.0, 34.1, 21.3, 13.2; HRMS (ESI-TOF, [M]⁺): calcd for C₂₃H₂₀N₂O₃, 372.1468; found, 372.1436.

12-(4-Methoxybenzoyl)-9,10-dihydrobenzo[e]pyrimido-[1,2-*a*]indol-5(8*H*)-one (3i'). Yellow solid, mp. 239–240 °C; IR (KBr) (ν_{max} , cm⁻¹): 3074 (w), 2964 (w), 2935 (w), 2852 (w), 1646 (w), 1602 (vs), 1506 (s), 1449 (w), 1402 (w), 1348 (m), 1249 (m), 1198 (w), 1159 (w), 1104 (w), 1033 (w), 919 (w), 837 (w), 770 (w); ^1H NMR (500 MHz, CDCl₃): 8.03 (m, 1H, ArH), 7.86 (m, 1H, ArH), 7.69–7.54 (m, 5H, ArH), 6.88 (m, 2H, ArH), 4.56 (m, 2H, CH₂), 3.87 (s, 3H, CH₃), 3.52 (m, 2H, CH₂), 2.21 (m, 2H, CH₂); ^{13}C NMR (125 MHz, CDCl₃) (δ , ppm): 190.9, 179.9, 174.8, 162.2, 149.9, 133.4, 133.1, 132.6, 130.8, 126.2, 126.0, 125.2, 113.0, 100.6, 55.2, 43.1, 38.0, 20.7; HRMS (ESI-TOF, [M + K]⁺): calcd for C₂₃H₁₈KN₂O₃, 409.0949; found, 409.1157.

(4-Chlorophenyl)(5-hydroxy-8,9,10,11-tetrahydrobenzo-[*e*]pyrimido[1,2-*a*]indol-12-yl)methanone (3i'). White solid, mp. 246–247 °C; IR (KBr) (ν_{max} , cm⁻¹): 3333 (s), 3290 (w), 2968 (w), 2866 (w), 1607 (vs), 1537 (s), 1469 (w), 1414 (m), 1359 (w), 1269 (w), 1218 (w), 1163 (m), 1053 (w), 1006 (w), 904 (w), 829 (w), 754 (w); ^1H NMR (500 MHz, CDCl₃+DMSO- d_6): 8.30 (s, 1H, OH), 8.20 (d, J = 7.6 Hz, 1H, ArH), 8.13 (d, J = 8.2 Hz, 1H, ArH), 7.58 (d, J = 8.2 Hz, 2H, ArH), 7.43 (d, J = 8.2 Hz, 2H, ArH), 7.40–7.37 (m, 1H, ArH), 7.25 (d, J = 7.0 Hz, 1H, ArH), 6.49 (s, 1H, ArH), 4.52–4.50 (m, 2H, CH₂), 3.54 (m, 2H, CH₂), 2.21–2.18 (m, 2H, CH₂); ^{13}C NMR (125 MHz, CDCl₃+DMSO- d_6) (δ , ppm): 187.2, 152.9, 148.6, 141.2, 135.7, 129.9, 129.0, 126.4, 124.2, 122.9, 122.6, 122.2, 121.9, 120.2, 101.8, 97.5, 45.0, 37.9, 22.0; HRMS (ESI-TOF, [M]⁺): calcd for C₂₂H₁₇ClN₂O₂, 376.0973; found, 376.0942.

Acknowledgements

This work was supported by the Program for Changjiang Scholars and Innovative Research Team in University (no. IRT13095), the National Natural Science Foundation of China (no. 81160384, 21162037, 21262042, U1202221, and 21362042), and the Reserve Talent Foundation of Yunnan Province for Middle-aged and Young Academic and Technical Leaders (no. 2012HB001).

Notes and references

- (a) P. A. Wender, *Nat. Prod. Rep.*, 2014, **31**, 433; (b) P. A. Wender and R. J. Ternansky, *Tetrahedron Lett.*, 1985, **26**, 2625.
- (a) M. B. Gawande, V. D. B. Bonifácio, R. Luque, P. S. Branco and R. S. Varma, *Chem. Soc. Rev.*, 2013, **42**, 5522; (b) R. A. Sheldon, *Chem. Soc. Rev.*, 2012, **41**, 1437; (c) P. Anastas and N. Eghbali, *Chem. Soc. Rev.*, 2010, **39**, 301.
- (a) J. Schranck, A. Tlili and M. Beller, *Angew. Chem. Int. Ed.*, 2013, **52**, 7642; (b) G. Vincent, in *Stereoselective Synthesis of Drugs and Natural Products*, ed. V. Andrushko and N. Andrushko, John Wiley & Sons, Hoboken, 2013, vol. 2, ch. 41, p. 1251; (c) C. Lamberth and J. Dinges, in *Bioactive Heterocyclic Compound Classes: Pharmaceuticals*, ed. C. Lamberth and J. Dinges, Wiley-VCH, Weinheim, 2012, ch. 1, pp. 3–5.
- (a) Y.-Z. Lin and X.-W. Zhan, in *Organic Optoelectronics*, ed. W.-P. Hu, Wiley-VCH, Weinheim, 2013, ch. 8, p. 381; (b) S. M. Bronner, G.-Y. J. Im and N. K. Garg, in *Heterocycles in Natural Product Synthesis*, ed. K. C. Majumdar and S. K. Chattopadhyay, Wiley-VCH, Weinheim, 2011, ch. 7, pp. 221–222; (c) Y.-J. Wu, *Top. Heterocycl. Chem.*, 2010, **26**, 1–29; (d) T. C. Barden, *Top. Heterocycl. Chem.*, 2010, **26**, 31–46.
- C.-H. Lu, Y.-Y. Li, J.-J. Deng, S.-R. Li, Y. Shen, H.-X. Wang and Y.-M. Shen, *J. Nat. Prod.*, 2013, **76**, 2175.
- (a) X.-B. Chen, X.-M. Liu, R. Huang, S.-J. Yan and J. Lin, *Eur. J. Org. Chem.*, 2013, 4607; (b) F.-C. Yu, R. Huang, H.-C. Ni, J. Fan, S.-J. Yan and J. Lin, *Green Chem.*, 2013, **15**, 453; (c) L.-J. Yang, S.-J. Yan, W. Chen and J. Lin, *Synthesis*, 2010, **20**, 3536.
- (a) L.-R. Wen, Q.-C. Sun, H.-L. Zhang and M. Li, *Org. Biomol. Chem.*, 2013, **11**, 781; (b) F.-C. Yu, S.-J. Yan, L. Hu, Y.-C. Wang and J. Lin, *Org. Lett.*, 2011, **13**, 4782; (c) C. Huang, S.-J. Yan, X.-H. Zeng, X.-Y. Dai, Y. Zhang, C. Qing and J. Lin, *Eur. J. Med. Chem.*, 2011, **46**, 1172; (d) S.-J. Yan, C. Huang, C.-X. Su, Y.-F. Ni and J. Lin, *J. Comb. Chem.*, 2010, **12**, 91.
- (a) Y.-C. Zhang, Z.-C. Liu, R. Yang, J.-H. Zhang, S.-J. Yan and J. Lin, *Org. Biomol. Chem.*, 2013, **11**, 7276; (b) C.-S. Yao, W.-H. Jiao, Z.-X. Xiao, Y.-W. Xie, T.-J. Li, X.-S. Wang, R. Liu and C.-X. Yu, *RSC Adv.*, 2013, **3**, 10801; (c) M. Li, P. Shao, S.-W. Wang, W. Kong and L.-R. Wen, *J. Org. Chem.*, 2012, **77**, 8956; (d) L.-R. Wen, C.-Y. Jiang, M. Li and L.-J. Wang, *Tetrahedron*, 2011, **67**, 293; (e) M. Li, Z.-M. Zhou, L.-R. Wen and Z.-X. Qiu, *J. Org. Chem.*, 2011, **76**, 3054; (f) L.-R. Wen, C. Liu, M. Li and L.-J. Wang, *J. Org. Chem.*, 2010, **75**, 7605.
- (a) J.-W. Gu, W.-T. Xiong, Z.-H. Zhang and S.-Z. Zhu, *Synthesis*, 2011, **21**, 1717; (b) S.-J. Yan, Y.-J. Liu, Y.-L. Chen, L. Liu and J. Lin, *Bioorg. Med. Chem. Lett.*, 2010, **20**, 5225.
- (a) M. Yaqub, R. Perveen, Z. Shafiq, H. Pervez and M. N. Tahir, *Synlett*, 2012, **23**, 1755; (b) S.-J. Yan, Y.-L. Chen, L. Liu, Y.-J. Tang and J. Lin, *Tetrahedron Lett.*, 2011, **52**, 465.
- (a) X.-B. Chen, Z.-C. Liu, L.-F. Yang, S.-J. Yan and J. Lin, *ACS Sustainable Chem. Eng.*, 2014, **2**, 1155; (b) X.-B. Chen, L. Zhu, L. Fang, S.-J. Yan and J. Lin, *RSC Adv.*, 2014, **4**, 9926; (c) F.-C. Yu, Z.-Q. Chen, X.-P. Hao, S.-J. Yan, R. Huang and J. Lin, *RSC Adv.*, 2014, **4**, 6110; (d) L.-R. Wen, Z.-R. Li, M. Li and H. Cao, *Green Chem.*, 2012, **14**, 707; (e) F.-C. Yu, S.-J. Yan, R. Huang, Y.-J. Tang and J. Lin, *RSC Adv.*, 2011, **1**, 596; (f) S.-J. Yan, Y.-L. Chen, L. Liu, N.-Q.

- He and J. Lin, *Green Chem.*, 2010, **12**, 2043.
- 12 (a) X.-B. Chen, X.-Y. Wang, D.-D. Zhu, S.-J. Yan and J. Lin, *Tetrahedron*, 2014, **70**, 1047; (b) A. Alizadeh, J. Mokhtari and M. Ahmadi, *Tetrahedron*, 2012, **68**, 319.
- 13 I. Koca, S. H. Ungoren, I. E. Kibriz and F. Yilmaz, *Dyes Pigm.*, 2012, **95**, 421.
- 14 For reviews on heterocyclic ketene amins, see: (a) K.-M. Wang, S.-J. Yan and J. Lin, *Eur. J. Org. Chem.*, 2014, 1129; (b) M.-X. Wang and Z.-T. Huang, *Prog. Nat. Sci.*, 2002, **12**, 249; (c) M.-X. Wang and Z.-T. Huang, *Prog. Nat. Sci.*, 1999, **9**, 971; (in Chinese) (d) Z.-T. Huang and M.-X. Wang, *Heterocycles*, 1994, **37**, 1233.
- 15 (a) C. D. Nenitzescu, *Bull. Soc. Chim. Romania*, 1929, **11**, 37; (b) L. Kürti and B. Czákó, in *Strategic Applications of Named Reactions in Organic Synthesis: Background and Detailed Mechanisms*, Elsevier, Burlington, 2005, p.312; (c) J.-J. Li, in *Name Reactions in Heterocyclic Chemistry*, John Wiley & Sons, Hoboken, 2005, ch. 9, p. 145; (d) J.-J. Li, in *Name Reactions: A Collection of Detailed Mechanisms and Synthetic Applications*, Springer, Cham, 2014, p. 432.
- 16 For recent studies and reviews on the Nenitzescu reaction, see: (a) P. A. Suryavanshi, V. Sridharan and J. C. Menéndez, *Tetrahedron*, 2013, **69**, 5401; (b) M. Inman and C. J. Moody, *Chem. Sci.*, 2013, **4**, 29; (c) U. Kucklaender, R. Bollig, W. Fran, A. Gratz and J. Jose, *Bioorg. Med. Chem.*, 2011, **19**, 2666; (d) M. Borthakur, S. Gogoi, J. Gogoi and R. C. Boruah, *Tetrahedron Lett.*, 2010, **51**, 5160; (e) V. S. Velezheva, A. I. Sokolov, A. G. Kornienko, K. A. Lyssenko, Y. V. Nelyubina, I. A. Godovikov, A. S. Peregudov and A. F. Mironov, *Tetrahedron Lett.*, 2008, **49**, 7106; (f) S. A. Patil, R. Patil and D. D. Miller, *Curr. Org. Chem.*, 2008, **12**, 691; (g) V. S. Velezheva, A. G. Kornienko, S. V. Topilin, A. D. Turashev, A. S. Peregudov and P. J. Brenna, *J. Heterocycl. Chem.*, 2006, **43**, 873; (h) G. R. Humphrey and J. T. Kuethe, *Chem. Rev.*, 2006, **106**, 2875; (i) J. Landwehr and R. Troschütz, *Synthesis*, 2005, **14**, 2414.
- 17 (a) V. Aggarwal, A. Kumar, H. Ila and H. Junjappa, *Synthesis*, 1981, 157; (b) Z.-R. Wang, in *Comprehensive Organic Name Reactions and Reagents*, John Wiley & Sons, Hoboken, 2010, ch. 458, p. 2038.
- 18 (a) W. Kohn, A. D. Becke and R. G. Parr, *J. Phys. Chem.*, 1996, **100**, 12974; (b) E. J. Baerends and O. V. Gritsenko, *J. Phys. Chem. A*, 1997, **101**, 5383; (c) Y. Zhao and D. G. Truhlar, *Acc. Chem. Res.*, 2008, **41**, 157; (d) J. P. Perdew, A. Ruzsinszky, L. A. Constantin, J.-W. Sun and G. Csonka, *J. Chem. Theory Comput.*, 2009, **5**, 902.
- 19 Based on the general procedure for the synthesis of compounds **3**, two products (**3b** and **3b'**) were produced simultaneously and their polarities are too similar to separate from the crude mixture by column chromatography. Therefore, HPLC must be used for the purification of compounds **3b** and **3b'**.
- 20 E. R. Johnson, S. Keinan, P. Mori-Sánchez, J. Contreras-García, A. J. Cohen and W. Yang, *J. Am. Chem. Soc.*, 2010, **132**, 6498.
- 21 M. J. Frisch, G. W. Trucks, H. B. Schlegel, G. E. Scuseria, M. A. Robb, J. R. Cheeseman, J. A. Montgomery, Jr., T. Vreven, K. N. Kudin, J. C. Burant, J. M. Millam, S. S. Iyengar, J. Tomasi, V. Barone, B. Mennucci, M. Cossi, G. Scalmani, N. Rega, G. A. Petersson, H. Nakatsuji, M. Hada, M. Ehara, K. Toyota, R. Fukuda, J. Hasegawa, M. Ishida, T. Nakajima, Y. Honda, O. Kitao, H. Nakai, M. Klene, X. Li, J. E. Knox, H. P. Hratchian, J. B. Cross, V. Bakken, C. Adamo, J. Jaramillo, R. Gomperts, R. E. Stratmann, O. Yazyev, A. J. Austin, R. Cammi, C. Pomelli, J. W. Ochterski, P. Y. Ayala, K. Morokuma, G. A. Voth, P. Salvador, J. J. Dannenberg, V. G. Zakrzewski, S. Dapprich, A. D. Daniels, M. C. Strain, O. Farkas, D. K. Malick, A. D. Rabuck, K. Raghavachari, J. B. Foresman, J. V. Ortiz, Q. Cui, A. G. Baboul, S. Clifford, J. Cioslowski, B. B. Stefanov, G. Liu, A. Liashenko, P. Piskorz, I. Komaromi, R. L. Martin, D. J. Fox, T. Keith, M. A. Al-Laham, C. Y. Peng, A. Nanayakkara, M. Challacombe, P. M. W. Gill, B. Johnson, W. Chen, M. W. Wong, C. Gonzalez and J. A. Pople, *Gaussian03, Revision D.01*, Gaussian, Inc., Wallingford CT, 2004.
- 22 P. C. Hariharan and J. A. Pople, *Theor. Chim. Acta*, 1973, **28**, 213.
- 23 (a) K. Fukui, *Acc. Chem. Res.*, 1981, **14**, 363; (b) C. Gonzalez and H. B. Schlegel, *J. Phys. Chem.*, 1990, **94**, 5523; (c) H. P. Hratchian and H. B. Schlegel, in *Theory and Applications of Computational Chemistry: The First Forty Years*, ed. C. E. Dykstra, G. Frenking, K. S. Kim and G. E. Scuseria, Elsevier, Amsterdam, 2005, pp. 195–249.
- 24 T. Lu and F. Chen, *J. Comput. Chem.*, 2012, **33**, 580.
- 25 W. Humphrey, A. Dalke and K. Schulten, *J. Mol. Graph.*, 1996, **14**, 33.
- 26 For the purpose of green chemistry, the alternative eluent, *n*-heptane–EtOAc (2:3, v/v) can be used for chromatographic purification.

TOC Graphic

An environmentally benign, mild, and catalyst-free reaction of quinones with heterocyclic ketene amins in ethanol: site-selective synthesis of rarely fused [1,2-*a*]indolone derivatives *via* an unexpected anti-Nenitzescu strategy

Bei Zhou,^{‡a} Zhi-Cheng Liu,^{‡a,b} Wen-Wen Qu,^b Rui Yang,^b Xin-Rong Lin,^a Sheng-Jiao Yan,^{*a} and Jun Lin^{*a}

The first site-selective methodology for the construction of fused [1,2-*a*]indolone derivatives *via* an unexpected anti-Nenitzescu strategy has been developed.

